Korean J. Chem. Eng., 40(12), 2982-2989 (2023)
DOI: 10.1007/s11814-023-1532-x

pISSN: 0256-1115
eISSN: 1975-7220

Polyurea membrane for water cleaning: Kinetic and equilibrium modeling of dyes adsorption

Pablo del Campo Calvo[*,], Lilian Karla de Oliveira[***], Nicole Aparecida Amorim de Oliveira[*], and Eduardo Ferreira Molina[*,†]**

*Universidade de Franca, Av. Dr. Armando Salles Oliveira 201, 14404-600 Franca-SP, Brazil
**Universidad Pública de Navarra, Av. Cataluña, 31006 Pamplona, Navarra, España
***Instituto Federal de São Paulo, Campus Barretos, Avenida C-1, 250, 14781-502 Barretos-SP, Brazil
(*Received 5 April 2023 • Revised 20 June 2023 • Accepted 12 July 2023*)

Abstract−The present treatment of water from aqueous solutions, reported from our research work, uses polyurea (PU) as a novel adsorbent. Specifically, the adsorption efficacy of PU was tested in dyes with different characteristics (Congo red (CR) and methylene blue (MB)). The PU membrane was obtained by a sol-gel chemistry reaction of polyetheramine with polyisocyanate resulting in the formation of urea groups, confirmed through FTIR analysis. The polymeric membrane exhibited a high homogeneity, making it a viable purifying technology for wastewater. The high swelling capacity of the membrane played a crucial role in the CR dye diffusion/adsorption. Notably, PU membranes showed excellent adsorption to CR anionic dye, resulting in a removal efficiency over 85%. However, MB dye adsorption was less favorable, suggesting a high affinity with anionic species. Our analysis revealed that the adsorption of CR dye onto PU membranes follows the pseudo-second order kinetic and Langmuir isotherm models. Moreover, the intraparticle diffusion model demonstrated that the swelling of PU facilitates the adsorption/diffusion process, thereby accelerating the mass transfer of the CR dye onto the membrane. Overall, our findings suggest that PU membranes derived from commercially available reagents are highly promising for the decontamination of dye wastewater.

Keywords: PEO, Urea Group, Congo Red, Methylene Blue, Swelling

INTRODUCTION

Industrial pollution by dyes is a pressing environmental issue due to the toxic and hazardous substances released during the manufacturing and dye-usage processes [1,2]. Dyes are widely applied in various industrial fields, such as textile, leather, plastics, paint and paper, for coloring and coating purposes [3]. This dye-related pollution can have adverse health effects, including skin irritation and respiratory problems. It can also disrupt aquatic ecosystems, as many dyes are readily biodegradable, and accumulate in the environment [4].

Traditional and biological wastewater treatment methods, are still inefficient to successfully remove dyes and pharmaceutical molecules from water due to their persistent and non-biodegradable nature [5]. So far, adsorption is the most cost-effective, efficient, and reliable technology for eliminating water-soluble toxic chemicals for wastewater treatment. The search for effective purification technologies is one of the most studied themes in both industrial and academic circles. Indeed, even a tiny amount of dye (1 mg L^{-1}) in wastewater discharge significantly detracts the aesthetic and transparency of water bodies, and can have an indirect, but far-reachin impact on aquatic life [6]. In general, dyes can be divided into three categories: cationic, anionic, and nonionic. The purpose of this study was to appraise the efficacy of a polyurea membrane (PU) in removing textile dyes.

Adsorbent dosage and contact time with the synthesized polyurea membrane were investigated from the study of two distinct dyes. The cationic methylene blue (MB) dye was first considered, after which the anionic Congo red (CR) dye. MB is a synthetic dye, primarily used as a biological stain with a characteristic deep blue color. CR, meanwhile, is a dye widely used in the textile industry. Being an anionic azo compound (dark red powder), it dissolves easily in water and forms a bright red solution. However, its chemical structure turns it high stable and toxic, which endangers the aquatic ecosystem and its marine organisms. Besides, the degradation of CR produces benzidine, a well-known carcinogenic compound, further underlining the serious concerns raised by its presence [7-9].

Polyurea (PU) are microphase-isolated structures formed of both soft and hard segments. They synthetized during the reaction polyisocyanates with polyamines [10]. PU membranes offer multiple advantages, including i) low-cost production, ii) the ability to fine tune the membrane thickness and shape, and iii) the possibility of obtaining them at room temperature without the use of a catalyst, thanks to the sol-gel process [11-13]. Due to their high durability, flexibility, resistance to climate and abrasion, they have found widespread use in industrial and commercial applications. Furthermore, polyurea membrane technology has great advantages as adsorbents such as insoluble in aqueous medium, not flocculate or agglomerate during dye adsorption process make possible the easy extraction of the membrane after adsorption from aqueous solution. In a recent study, Yu et al. [14] successfully synthesized porous polyurea microspheres using isophorone diisocyanate (IPDI), trieth-

†To whom correspondence should be addressed.
E-mail: eduardo.molina@unifran.edu.br

ylenetetramine (TETA), and SiO_2 particles. The team conducted tests on the adsorbent's ability to remover methyl orange (MO) and iodine from water, which demonstrated the potential of cross-linked polyurea-derivated material for water purification applications. Dsouza et al. [15] reported the potential of ordered polyurea films for the adsorption of fluorescent dyes. Thanks the urea groups, which enabled hydrogen bonding with dye molecules, the membrane exhibited promising results for the selective transport of various organic molecules. On the base of this research, we hereby present the first application of a polyurea membrane based on polyetheramine-PEO and polyisocyanate crosslinker (hexamethylene diisocyanate trimer) as an adsorbent for dye removal from aqueous solutions. To ensure the utmost accuracy and precision of our findings, we investigated the homogeneity of the membranes through the powerful Fourier-transform infrared spectroscopy (FTIR). To a better understanding of the swelling degree of the final materials, we compared different aqueous medium as water, MB and CR dye aqueous solutions. We also explored the adsorption properties and mechanism toward dye molecules. To the best of our knowledge, the use of this class of polyurea is an unprecedented water purification process. Furthermore, the straightforward synthesis of the polyurea membrane by sol-gel chemistry at room temperature opens the door for large-scale production.

EXPERIMENTAL SECTION

1. Materials

Methylene Blue (MB) $C_{16}H_{18}ClN_3S$ and Congo Red (CR) $C_{32}H_{22}N_6Na_2O_6S_2$ were purchased from Sigma-Aldrich. Desmodur N3300, known as hexamethylene diisocyanate trimer-HDI (molecular weight=504 g mol^{-1}) and the O,O′-bis-(2-aminopropyl)polypropylene glycol-block-polyethylene glycol-block-polypropylene (PEO with a molecular weight=1,900 g mol^{-1}) were donated by Bayer Corporation and Huntsman Performance Products (Brazil), respectively.

2. Polyurea Membrane Synthesis

PU membranes were prepared using a previously reported sol-gel procedure in literature [10-13]. Briefly, the HDI was covalently bonded to the polyether backbone of PEO by the reaction of the -N=C=O and the NH_2 groups attached to the end of the polyether. 4 g of polyether-PEO and 1 g of HDI were dissolved separately in two beakers containing acetone. The beakers were sealed and stirred for two hours at room temperature to produce homogenous solutions. The HDI solution was then added dropwise to the PEO solution while stirring at room temperature until the complete dissolution was achieved (see Scheme 1). The resulting solution was then poured into a flask and left to gel for 1 day at 25 °C.

3. Characterization

FTIR spectra were obtained at room temperature in the 400-3,000 cm^{-1} range by averaging 32 scans with a spectral resolution of 2 cm^{-1} using a Perkin Elmer Spectrometer Frontier and the ATR accessory. The swelling capacity of the PU membrane (~850 mg and 3 mm thick) was studied by gravimetric method. The membrane was immersed in the aqueous medium (at room temperature) and after the predetermined time, the swollen samples carefully removed from the aqueous medium, dried between two filter papers to remove any excess water on the surface, and weighed on an electronic analytical balance. The swelling ratio (S) was determined using the Eq. (1):

$$S = \frac{Ws - Wd}{Wd} * 100 \quad (1)$$

where Ws and Wd are the mass of swollen and dry samples, respectively. The aqueous medium used for the swelling assays were pure water, MB and CR solution. The experiments were conducted using three separate samples, and the results displayed are data mean.

4. Adsorption Studies

To assess the interaction of PU and contaminants with different characteristics, adsorption studies were carried out using MB and CR dyes. Stock solutions of 100 mg L^{-1} were prepared by dissolving 50 mg of dye (MB or CR) in 500 mL of water and then diluted to several concentrations. For kinetic assays, PU membrane (850 mg) were poured to 50 mL of 20 mg L^{-1} MB or CR dye aqueous solution under constant stirring. To understand the diffusion process of dye molecules in membranes, the kinetic tests using CR organic dye were driven using different dosage of PU (850, 450 and 220 mg). The experiments occured for 2 days (2,880 minutes) at 25 °C and natural pH (~7.0). For the equilibrium experiment, 200 mg of the PU membrane was added in 50 mL of an aqueous CR solution containing a dye concentration in the range of 5 to 50 mg L^{-1}. The system was maintained static for 24 h at 25 °C. Adsorption capacity values at different times (q_t) were determined as follows:

$$q_t = \frac{(Ci - Cf)}{m} \times V \quad (2)$$

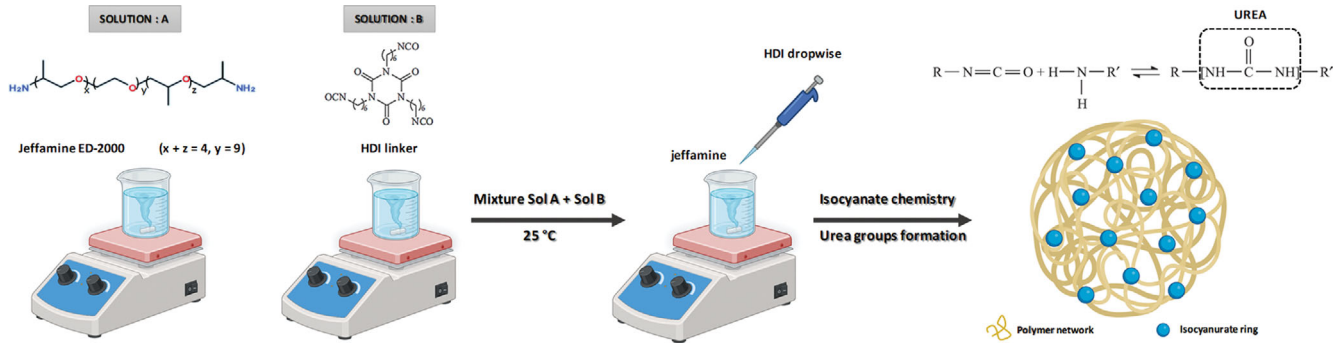

Scheme 1. General synthetic route for the preparation of polyurea membrane.

where Ci and Cf (mg L^{-1}) are the initial and final concentrations of CR dye, respectively, V (L) is the volume of the solution, and m (g) is the mass of PU membrane.

The dye concentration was determined using UV-vis spectroscopy (Agilent Technologies Cary 60 model), which was equipped with a fiber-optic, solarization-resistant immersion probe. Standard aqueous MB and CR solution in range of 0-50 mg L^{-1} were used to build the calibration curves, with a λ_{max} of 665 nm and 498 nm, respectively.

RESULTS AND DISCUSSION

The FTIR analysis conducted on the PU membrane investigated thoroughly the formation of the -NH- from urea groups. Fig. 1(a) depicts the five points analyzed, along with the corresponding FTIR spectrum. Reference to literature [16,17], the HDI component presents a peak at 2,266 cm^{-1} due to isocyanate groups. The absence of this peak in the polyurea membrane along all five points analyzed signals the successful formation of a structure containing urea groups connected to the hard domains of the matrix. Additionally, the presence of the peaks at 1,636 cm^{-1} and 1,560 cm^{-1}, attributed to C=O amide I, and CO-N-H amide II, respectively, evidences the formation of urea groups (Fig. 1(b)). In the range of 1,300-700 cm^{-1}, the FTIR spectrum ascribes, the characteristic peaks at ~1,140, 1,100, 950 and 845 cm^{-1} to the CH_2 and C-O-C from PEO backbone [18-20]. In other words, the FTIR analysis confirms the homogeneity of the PU membrane throughout the obtained area and the data collected for three different polyurea showed similar results, demonstrating the high reliability of the sol-gel method for the production of these membranes.

Assessing the extent of swelling (water absorption) is an essential feature of membranes, as it is largely determined by their overall structure. Monitoring this property can help to understand a membrane's hydrophilicity. To measure of the swelling capacity (S) of the PU membrane, the samples were immersed in three different solutions and the augment in the PU mass monitored. Fig. 2 depicts a relatively high swelling degree, reaching 195% in CR dye solution. Both CR and MB dye solutions yielded similar results (see red squares and blue pentagons in Fig. 2). The swelling degree with distilled water decreased slightly to 175% (gray circles, Fig. 2). These results suggest that the PU membrane immersed in an aqueous solution containing dye molecules, is affected by the presence of the dye, thus leading to an increase in the swelling degree.

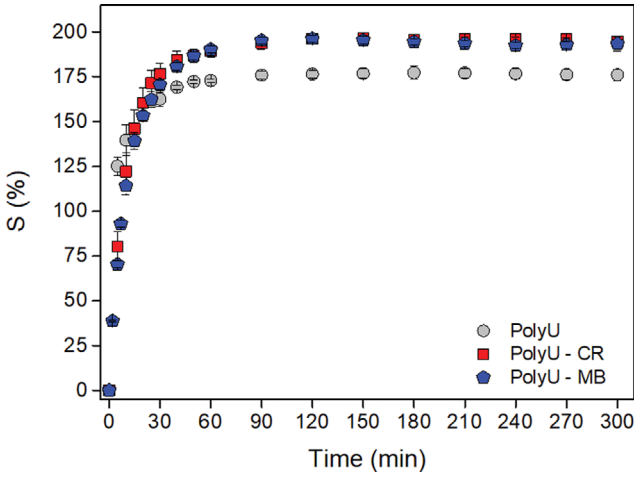

Fig. 2. Temporal evolution of swelling degree of PU using different aqueous medium: water, MB and CR solution. The concentration of both dye solutions was 20 mg L^{-1}.

For the understanding of the adsorption behavior, kinetic assays are essential. The data gained from contact time experiments gleaned valuable insights regarding the equilibrium time of the adsorption process, specifically the duration required for the adsorption and desorption process to reach a steady state. Fig. 3, showcase the data obtained from a contact time experiment using a PU membrane and two dyes: cationic MB (a) and anionic CR (b). It is worth to note that the MB concentration steadily increases over the time after its interaction with membrane, while the CR solution concentration decreases rapidly upon contact with PU. Thus, there is a high affinity of the PU adsorbent with anionic species, while they have

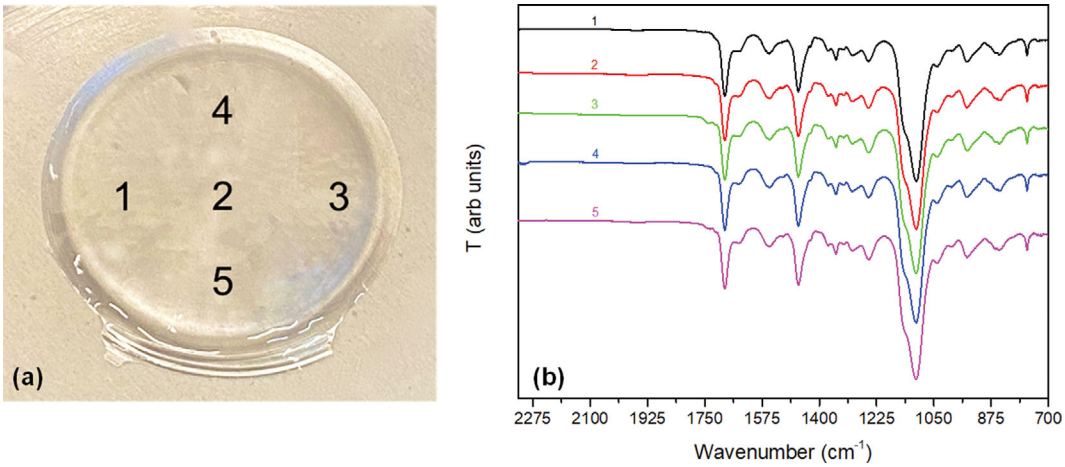

Fig. 1. (a) Photograph of polyurea membrane highlighting the five points analyzed by FTIR, and (b) polyurea FTIR spectrum collected in each point.

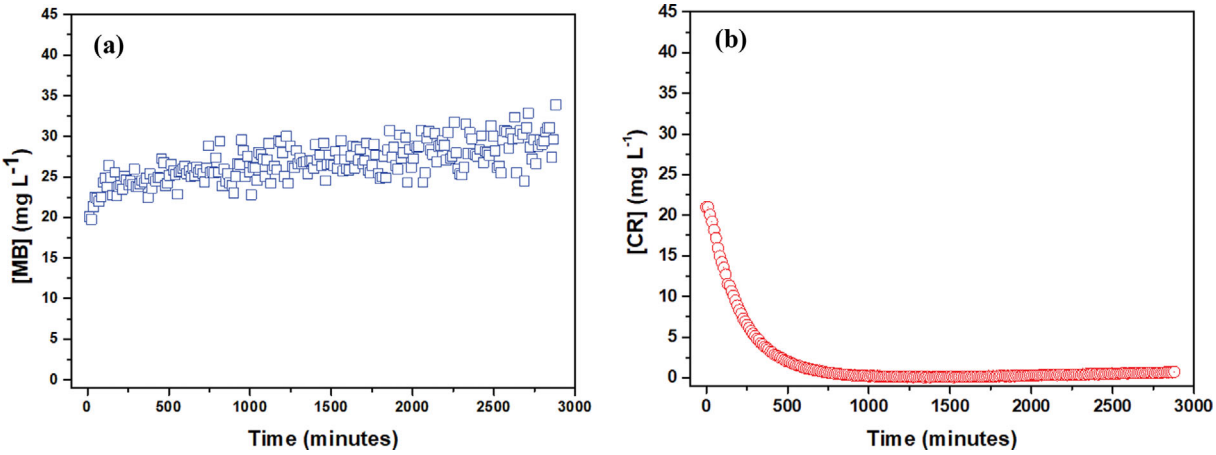

Fig. 3. Evaluation of the PU membrane and MB (a) and CR dyes (b) in 20 mg L^{-1} concentration and at 25 °C.

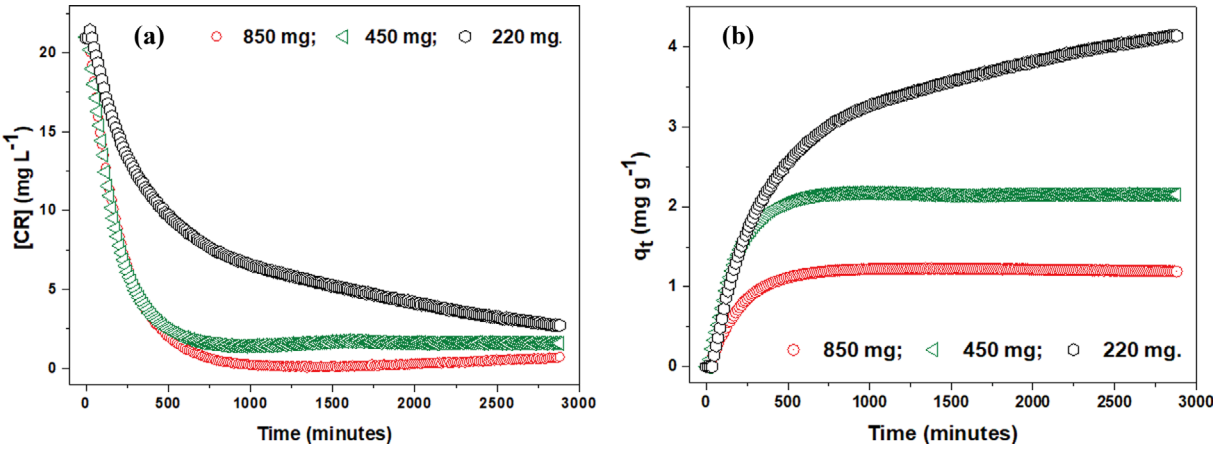

Fig. 4. (a) Temporal evolution of CR concentration in solution using various masses of PU membrane; (b) CR adsorption capacity onto PU with different masses of membrane.

a weak interaction with cationic molecules due to their low affinity with the urea groups in membrane, as demonstrated in FTIR characterization. The increase of MB solution concentration could be explained for the process of water uptake of the membrane, as visualized in the swelling test using water, MB and CR solution. The PU membrane swelling started before the adsorption process and helped the diffusion of the dye's molecules. However, the MB dye had no affinity with the active sites of PU membrane and as foreseen Fig. 3(a), it is expected that high water absorption by PU network following by rejection of MB adsorption leads to a concentrated MB aqueous solution.

Experiments using different masses of PU membrane were conducted to understand how the diffusion of the CR dye molecules affects the adsorption process (Fig. 4(a)). It appears clearly that the CR concentration in solution depended on the PU mass used in the test, while the adsorption capacity augmented with contact time regardless of the PU mass used (Fig. 4(b)). The efficacy of CR dye removal from water solution by adsorption was initially rapid and then gradually slowed down until it reached equilibrium. The experiments using 850 and 450 mg of PU required an equilibrium time of 500 minutes (~8 hours), whereas it was not possible to distinguish an equilibrium time of the kinetic assay using 220 mg of PU. This difference could be attributed to the availability of PU active sites, as higher mass values the PU samples have more available active sites that facilitate the diffusion of CR molecules onto adsorbent. The kinetic results of the CR adsorption onto PU membranes suggested that the significant impact of swelling time of membrane in the process. This observation is in adequation with the equilibrium time reported by Lian et al. [21] where they evaluated the CR adsorption onto organoclay. These results underscore the importance of carefully considering the swelling time when designing and optimizing membrane-based adsorption systems.

After 48 h, the CR concentration in the supernatant was 0.72, 1.59 and 2.70 mg L^{-1} in tests using 850, 450 and 220 mg of PU membrane, respectively. Thereby, the process showed a clear efficiency in cleaning water at a rate higher than 85%. To clarify the processes involved in CR adsorption onto a PU membrane, we fitted the data acquired from contact time experiments to pseudo-first and pseudo-second order kinetic models. Eqs. (3) and (4) correspond to non-linear forms of these models, respectively.

$$q_t = q_{eq}(1 - e^{K_1 t}) \quad (3)$$

Table 1. Comparison of adsorption constants of the CR dye onto PU membrane obtained using kinetic models

		Pseudo-first order			Pseudo-second order		
PU dosage (mg)	$q_{eq\ experimental}$†	k_{1}†	$q_{eq\ calculated}$†	R^2	k_{2}†	$q_{eq\ calculated}$†	R^2
850	1.20	7.00×10^{-3}	1.86	0.935	9.90×10^{-3}	1.26	0.995
450	2.16	2.33×10^{-3}	2.62	0.732	6.24×10^{-3}	2.23	0.996
220	4.14	1.50×10^{-3}	4.20	0.857	3.99×10^{-4}	4.85	0.988

†q_{eq}=amounts of CR (mg g^{-1}) adsorbed at equilibrium; k_1=the pseudo-first order rate constant (min^{-1}); k_2=the pseudo-second order rate constant (mg g^{-1} min^{-1}).

$$q_t = \frac{K_2 q_{eq}^2 t}{1 + K_2 q_{eq} t} \quad (4)$$

where q_{eq} and q_t are the amounts of CR dye (mg g^{-1}) adsorbed at equilibrium and at each time, respectively; t is the time (minutes); k_1 is the pseudo-first order rate constant (min^{-1}); and k_2 is the pseudo-second order rate constant (mg g^{-1} min^{-1}).

Table 1 presents the data obtained using the assessed kinetic models for different PU masses. Higher correlation coefficient values (R^2) were observed for the pseudo-second order kinetic model (R^2>0.98), and the q_{eq} calculated by pseudo-second order model values were in agreement with q_{eq} obtained experimentally. The results denoted that the number of active sites on the PU surface and the concentration of the CR dye were important factors in the rate of adsorption. Consequently, chemisorption was identified as the mechanism involved in the CR adsorption process, which occurs via the sharing or exchange of electrons between the adsorbent and the adsorbate. [22-24]. Cai et al. [25] evaluated the CR adsorption onto biosorbent and verified that pseudo-second order kinetic model best describes the adsorption process.

The adsorption of CR onto PU is linked to the rate of transport of dye molecules onto the adsorbent surface, as well as the rate of swelling of PU. Thus, we employed the intraparticle diffusion model (Eq. (5)) to better understand the mass transfer in the adsorption process [26].

$$q_t = k_d t^{0.5} + l \quad (5)$$

where k_d is the intraparticule diffusion rate constant (g^{-1} mg^{-1} $minutes^{-0.5}$) and l is a constant related to the diffusion boundary layer (mg g^{-1}).

Fig. 5 is the plot of q_t versus $t^{0.5}$ for the intraparticle diffusion model. As clearly observed, the adsorption process of dye onto membrane could be described from three different stages, as explained below. In a first stage, the occurrence of two different process could be identified: (i) membrane water uptake and (ii) diffusion of dye on PU. These processes were in synergy, as the membrane water absorption caused quickly transfer of CR molecules onto PU surface after immersion in the dye solution. During the second stage, the diffusion of dye molecules on surface PU decreased due the slow membrane water uptake. However, the diffusion rate of CR was faster in the second stage than in the subsequent one (third stage), where the adsorption rate decreases, and the system reached equilibrium. These findings are consistent with the literature that have evaluated the adsorption of organic contaminants onto organic-inorganic hybrid materials [27,28].

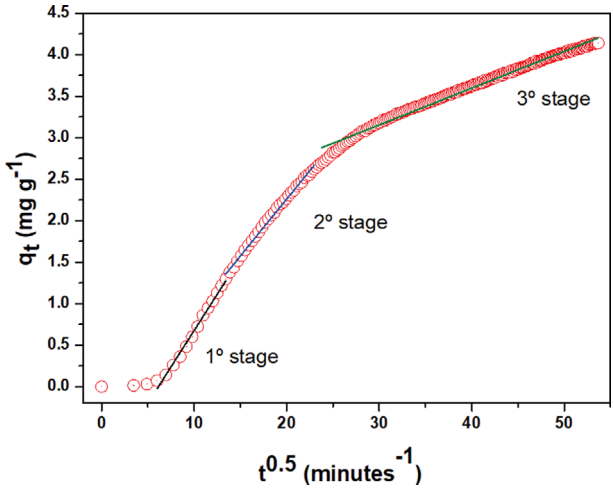

Fig. 5. Intraparticle diffusion model of CR dye adsorption on PU membrane using 220 mg of adsorbent.

The Table 2 lists the constants obtained using the intraparticle diffusion model for the CR adsorption on membrane using three different masses of PU. The diffusion rate constant (k_d) followed the order: k_{d1}>k_{d2}>k_{d3} independent of the PU mass employed in the adsorption process. Lower k_d values were observed in the experiments using 850 mg, possibly due to higher number of availability and accessibility of active sites on PU surface, enabling a faster occu-

Table 2. Intraparticle diffusion model constants for adsorption process of CR onto PU membrane

Mass (mg)	Intraparticle diffusion model								
	k_{d1}	l_1	R_1^2	k_{d2}	l_2	R_2^2	k_{d3}	l_3	R_3^2
850	0.0761	−0.346	0.999	0.0380	0.283	0.982	0.0122	0.860	0.970
450	0.152	−0.722	0.992	0.101	0.0275	0.986	0.0406	1.13	0.957
220	0.175	−1.07	0.991	0.137	−0.480	0.995	0.0443	1.83	0.987

k_d=intraparticle diffusion rate constant (g^{-1} mg^{-1} $min^{-0.5}$); l=constant related to the diffusion boundary layer (mg g^{-1}).

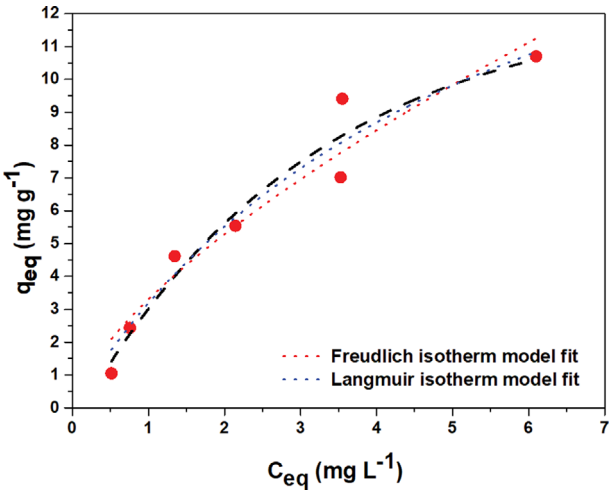

Fig. 6. Adsorption isotherm of CR dye onto PU membrane at 25 °C.

Table 3. Isotherms adsorption constants of CR adsorption onto PU membrane

T/°C	Langmuir isotherm model			Freundlich isotherm model		
25	q_{max}	K_L	R^2	K_F	n	R^2
	20.5	0.184	0.939	3.30	1.47	0.919

K_L=adsorption equilibrium constant (L mg^{-1}); q_{max}=maximum adsorption capacity (mg g^{-1}); n and K_F=Freundlich adsorption constant.

pation of the dye molecules. The diffusion process is in line with the results obtained, in which the fastest step of the adsorption was evidenced in the first stage. The diffusion boundary layer values (l) decreased in the order: $l_3>l_2>l_1$, indicating that the CR molecules are transferred to PU membrane until the adsorption process reached equilibrium.

Seven different concentrations of CR (ranging from 5 to 50 mg L^{-1}) were selected to examine the impact of the initial concentration on the adsorption process (Fig. 6). The experiments were carried out in natural pH (~7.0) at 25 °C. The increase of initial concentration caused a greater amount of CR on PU membranes *i.e.*, higher adsorption capacity values were observed with the increase of the initial dye concentration.

To further investigate the adsorption process, Langmuir (6), Freundlich (7) [29,30] isotherm models were used to fit the isothermal data.

$$q_{eq}=\frac{K_L q_{max} C_{eq}}{1+K_L C_{eq}} \quad (6)$$

$$q_e=K_F(C_{eq})^n \quad (7)$$

where q_{eq} and C_{eq} are the adsorption capacity (mg g^{-1}) and CR concentration (mg L^{-1}) at equilibrium, respectively. K_L is the adsorption equilibrium constant (L mg^{-1}); q_{max} is the theoretical maximum adsorption capacity (mg g^{-1}); n is Freundlich adsorption constant related to adsorption strength, and K_F is Freundlich constant related to the adsorption capacity (mg g^{-1})(L g^{-1})$^{1/n}$.

Table 3 displays the constants obtained using the Langmuir and

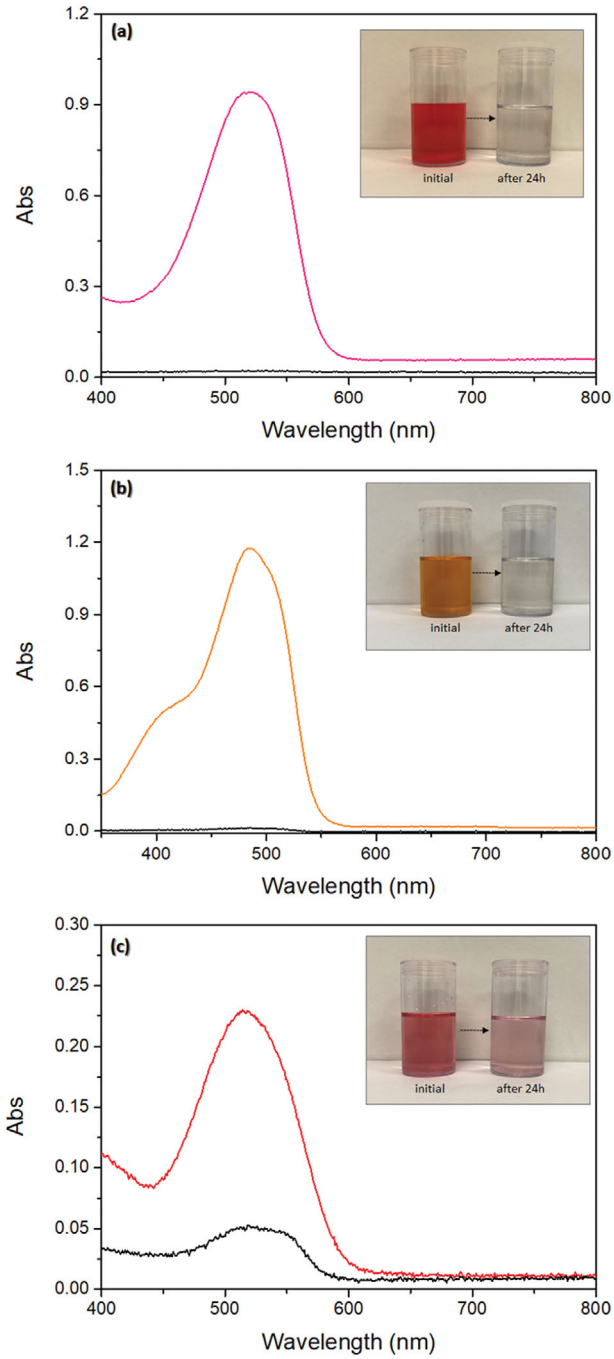

Fig. 7. UV-vis absorption spectra of the anionic dyes (a) Ponseau S, (b) Orange II and (c) Acid Red before and after contact with polyurea after 24 h. Inset: Photograph of (a) PS, (b) OII and (c) AR initial dye solution and after adsorption by polyurea membrane for 24 h. Mass of polyurea xerogel used was ~850 mg and initial dye concentration=20 mg L^{-1}.

Freundlich isotherm model. From the correlation coefficients values (R^2>0.93) the isotherm model that better described the CR adsorption onto PU was Langmuir model. This model suggests a monolayer adsorption. Similar results have been observed from literature using different adsorbent-based materials [31].

We have estimated the cost of producing a polyurea membrane

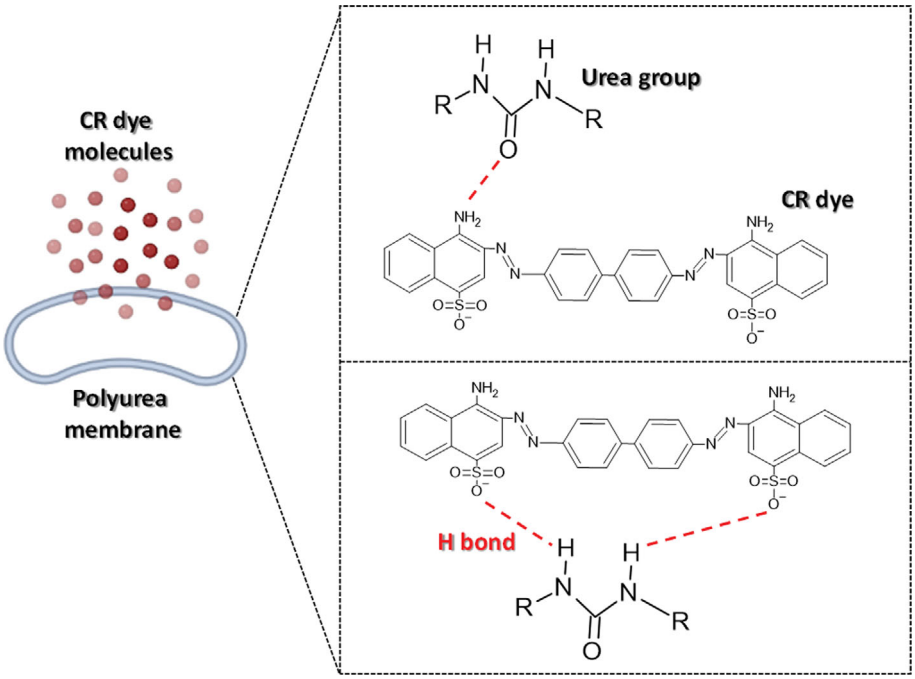

Fig. 8. Proposed mechanism for CR dye adsorption on polyurea membrane.

based on the commercially available reagents (PEO, Desmodur N3300, and acetone) used during the synthesis procedure. The summation of each elements was approximately 0.65 USD to obtain a polyurea membrane with the average thickness 2.0 mm±0.10 and diameter of 370 mm±0.05. Such a cost-effective preparation is a promising opportunity for engineering scale up.

To expand the application of the polyurea membranes to anionic dye removal we used a fragment of the xerogel in solutions of three other dyes such as Ponceau S (PS), Acid Red (AR) and Orange II (OII). Regardless of dye structure, after addition of polyurea (about 850 mg) for 24 h, the color of PS, AR and OII solutions turned obviously clearer (inset Fig. 7(a)-(c)), while, the PS, AR and OII characteristic UV-vis band became too weak to be observed, suggesting a high level efficacy in removing these anionic species (Fig. 7(a)-(c)). The UV-vis spectra of Fig. 7 (initial dye solution and after contact with polyurea) revealed a strong host-guest interaction of the membranes with different hydrophilic anionic dyes in aqueous solution.

Fig. 8 illustrates the proposed mechanism for CR adsorption on polyurea. As can be seen, the interaction between the adsorbent and adsorbate takes place through hydrogen bonds. Hydrogen bonds are formed through the electrostatic attraction between hydrogen and electronegative atoms such as nitrogen or oxygen [9]. The chemical structure of polyurea possess a higher content of nitrogen and oxygen, which enables easy binding with CR molecules.

The maximum monolayer adsorption capacities (q_{max}) of the polyurea membrane with other adsorbents is presented in Table 4. As indicated, q_{max} (mg g^{-1}) of the polyurea adsorbent is higher than previously reported works, which means that it can be an effective adsorbent for CR removal.

The literature has been highlighted the importance of the preparation of novel membrane-based materials with efficient performance for water filtration/separation [39,40]. In this work, polyurea membrane technology has great advantages as adsorbents such as insoluble in aqueous medium, flexible, transparency, high stability, not flocculate or agglomerate during dye adsorption process make possible the easy extraction of the membrane after adsorption from aqueous solution. This work gave us fundamental clues for the design and applications of this class of polyurea, such as in the precision separation of cationic/anionic dyes from aqueous solution.

Table 4. Comparison of the maximum monolayer adsorption capacities of the polyurea membrane with other reported CR adsorbents

Adsorbent	q_m (mg g^{-1})	Reference
Polyurea membrane	20.5	This work
Chitosan-coated quartz sand	3.50	32
Fly ash	13.46	33
Amino-functionalized silica gel	11.00	34
Tunics of the corm of the saffron	6.20	35
Kaolin	5.94	36
Water hyacinth stem carbon	13.44	37
Palygorskite	2.73	38

CONCLUSIONS

A low cost and scalable polyurea membrane was obtained by sol-gel process at room temperature. The membrane resulting material can be readily extended to remove other anionic dyes and open a wide range of possibilities to modification for purification technology such as selective separation of dyes from aqueous solution.

PU membrane demonstrated a remarkable removal efficiency of over 85% for the dye CR, while also demonstrating a hydrogel characteristic by taking up to 175% of its original mass in water. This work highlights a facile and cost-effective preparation of polyurea membranes, provides valuable insights for precise separation of cationic/anionic dyes from aqueous solution, as well as the expanding perspectives for the removal from wastewaters of pharmaceutical, metal species and so on.

ACKNOWLEDGEMENTS

We are grateful to Huntsman Performance Products and Bayer Group for their generous donation of Jeffamine® and triisocyanate crosslinker reagents, respectively. This research was funded by FAPESP grant nº 2021/06552-1, CAPES - Finance Code 001, and CNPq nº 307696/2021-9.

Conflicts of interest: There are no conflicts to declare.

REFERENCES

1. R. Jana, A. Gupta, R. Choudhary and O. P. Pandey, *J. Sol-Gel Sci. Technol.*, **96,** 405 (2020).
2. M. Jose, M. Kumari, R. Karunakaran and S. Shukla, *J. Sol-Gel Sci. Technol.*, **75**, 541 (2015).
3. N. Singh, S. Riyajuddin, K. Ghosh, S. K. Mehta and A. Dan, *ACS Appl. Nano Mater.*, **2**, 7379 (2019).
4. P. Rajapaksha, R. Orrell-Trigg, Y. B. Truong, D. Cozzolino, V. K. Truong and J. Chapman, *Environ. Sci. Adv.*, **1**, 456 (2022).
5. A. Huang, M. Yan, J. Lin, L. Xu, H. Gong and H. Gong, *Int. J. Environ. Res. Public Health*, **18**, 4909 (2021).
6. M. M. Tarekegn, R. M. Balakrishnan, A. M. Hiruy and A. H. Dekebo, *RSC Adv.*, **11**, 30109 (2021).
7. J. Shu, Z. Wang, Y. Huang, N. Huang, C. Ren and W. Zhang, *J. Alloys Compd.,* **633**, 338 (2015).
8. Y. Y. Chen, S. H. Yu, H. F. Jiang, Q. Z. Yao, S. Q. Fu and G. T. Zhou, *Appl. Surf. Sci.*, **444**, 224 (2018).
9. Y. Zheng, B. Cheng, J. Fan, J. Yu and W. Ho, *J. Hazard. Mater.*, **403**, 123559 (2021).
10. A. Shinko, S. C. Jana and M. A. Meador, *RSC Adv.*, **5**, 105329 (2015).
11. A. Sanchez-Ferrer, D. Rogez and P. Martinoty, *Macromol. Chem. Phys.*, **211**, 1712 (2010).
12. M. A. de Resende, G. A. Pedroza, L. H. G. M. C. Macêdo, R. Oliveira, M. Amela-Cortes, Y. Molard and E. F. Molina, *J. Appl. Polym. Sci.*, **139**, 51970 (2022).
13. G. A. Pedroza, L. H. G. M. C. Macêdo, R. Oliveira, N. N. Silveira, R. P. Orenha, R. L. T. Parreira, R. A. Santos, Y. Molard, M. Amela-Cortes and E. F. Molina, *J. Drug Deliv. Sci. Technol.*, **76**, 103744 (2022).
14. B. Yu, Y. Luo, H. Cong, C. Gu, W. Wang, C. Tian, J. Zhai and M. Usman, *RSC Adv.*, **6**, 111806 (2016).
15. R. Dsouza, D. Sriramulu and S. Valiyaveettil, *RSC Adv.*, **6**, 24508 (2016).
16. J. Mattia and P. Painter, *Macromolecules*, **40**, 1546 (2007).
17. A. Sánchez-Ferrer, V. Soprunyuk, M. Engelhardt, R. Stehle, H. A. Gilg, W. Schranz and K. Richter, *ACS Appl. Polym. Mater.*, **3**, 4070 (2021).
18. V. Z. Bermudez, L. D. Carlos and L. Alcacer, *Chem. Mater.*, **11**, 569 (1999).
19. M. Paredes, S. H. Pulcinelli, C. Peniche, V. Gonçalves and C. V. Santilli, *J. Sol-Gel Sci. Technol.*, **72**, 233 (2014).
20. N. A. M. de Jesus, A. H. P. de Oliveira, D. C. Tavares, R. A. Furtado, M. L. A. Silva, W. R. Cunha and E. F. Molina, *J. Sol-Gel Sci. Technol.*, **88**, 192 (2018).
21. L. Lian, L. Guo and C. Guo, *J. Hazard. Mater.*, **161**, 126 (2009).
22. Y. S. Ho, *J. Hazard. Mater.*, **136**, 681 (2006).
23. Y. S. Ho and G. McKay, *Water Res.*, **34**, 735 (2000).
24. Y. S. Ho and G. McKay, *Process Saf. Environ. Prot.*, **76**, 332 (1998).
25. T. Cai, H. Chen, L. Yao and H. Peng, *Int. J. Mol. Sci.*, **24**, 684 (2023).
26. W. J. J. Weber, Kinetics of adsorption of carbon from solution. In: J. C. Morris (Hrsg.). Journal of the Sanitary Engineering Division, American Society of Civil Engineers. Sanitary Engineering Division 31-59 (1963).
27. L. K. de Oliveira, A. L. A. Moura, V. Barbosa, R. L. T. Parreira, R. S. Banegas, G. F. Caramori, K. J. Ciuffi and E. F. Molina, *Environ. Sci. Pollut. Res.*, **24**, 18421 (2017).
28. A. L. A. Moura, L. K. de Oliveira, K. J. Ciuffi and E. F. Molina, *J. Mater. Chem. A*, **3**, 16020 (2015).
29. I. Langmuir, *J. Am. Chem. Soc.*, **40**, 1361 (1918).
30. H. M. F. Freundlich, *J. Phys. Chem.*, **57**, 385 (1906).
31. S. Tang, D. Xia, Y. Yao, T. Chen, J. Sun, Y. Yin, W. Shen and Y. Peng, *J. Colloid Interface Sci.*, **554**, 682 (2019).
32. T. Feng, F. Zhang, J. Wang and L. Wang, *J. Appl. Polym. Sci.*, **125**, 1766 (2012).
33. M. Harja, G. Buema and D. Bucur, *Sci. Rep.*, **12**, 6087 (2022).
34. R. S. Farias, H. L. B. Buarque, M. R. Cruz, L. M. F. Cardoso, T. A. Gondim and V. R. Paulo, *Eng. Sanit. E Ambient.*, **23**, 1053 (2018).
35. A. Dbik, S. Bentahar, M. E. Khomri, N. E. Messaoudi and A. Lacherai, *Mater. Today: Proc.*, **22**, 134 (2020).
36. B. Meroufel, O. Benali, M. Benyahia, Y. Benmoussa and M. A. Zenasni, *J. Mater. Environ. Sci.*, **4**, 482 (2013).
37. A. Extross, A. Waknis, C. Tagad, V. V. Gedam and P. D. Pathak, *Int. J. Environ. Sci. Technol.*, **20**, 1607 (2023).
38. A. B. F. Câmara, R. V. Sales, C. V. S. Júnior, M. A. F. de Souza, C. Longe, T. M. Chianca, R. D. Possa, R. C. Bertolino and L. S. Carvalho, *Korean J. Chem. Eng.*, **39**, 1805 (2022).
39. P. Marín San Román and R. P. Sijbesma, *Adv. Mater. Interfaces*, **9**, 2200341 (2022).
40. P. Marin San Roman, K. Nijmeijer and R. P. Sijbesma, *J. Membr. Sci.*, **644**, 120097 (2022).